Biomimetic and Technomimetic Single Molecular Machines

Claire Kammerer, Guillaume Erbland, Yohan Gisbert, Toshio Nishino, Kazuma Yasuhara, Gwénaël Rapenne

Biomimetic and Technomimetic Single Molecular Machines

Claire Kammerer,[1] Guillaume Erbland,[1] Yohan Gisbert,[1] Toshio Nishino,[2] Kazuma Yasuhara[2] and Gwénaël Rapenne*[1,2]

[1] CEMES, Université de Toulouse, CNRS, Toulouse, France

[2] Division of Materials Science, Nara Institute of Science and Technology, NAIST, 8916-5 Takayama-cho, Ikoma, Nara 630-0192, Japan

E-mail: gwenael-rapenne@ms.naist.jp

Abstract

This highlight review describes our contribution to the field of biomimetic and technomimetic molecular machines specially designed to be studied as single molecules on surfaces. Prototypes of molecular wheels, vehicles, gears and motors will be described from their design to the study of their controlled motions using ultra-high-vacuum low-temperature scanning tunneling microscopes (UHV-LT-STM).

Post-print

Published : *Chem. Lett.* **2019**, *48*, 299-308.

Introduction

A machine (latin *machina*, which itself comes from the ancient Greek *mekkanê*, meaning: ingenious invention, device, trick) is a complex manufactured object capable of using a source of energy to perform on its own or under the guidance an operator, one or more specific tasks.

Molecular machines have not been invented by mankind, they have existed for a very long time in Nature. Biological molecular machines are of formidable efficiency and are at the origin of various complex biological processes necessary for the functioning and survival of living organisms. A molecular-level machine can be defined as a molecule or an assembly of molecular components designed to perform a precise function in response to a controlled stimulus. This active field of research has been recently highlighted with the 2016 Nobel Prize of Chemistry awarded to J.-P. Sauvage, Sir J. F. Stoddart and B. L. Feringa for their seminal contributions to "the design and synthesis of molecular machines"[1] which revolutionized the way chemists think about molecular systems and their motions. Their remarkable achievements opened the door to a new dimension of chemistry with the control of motions at the molecular level, the molecular world moved from a static library to a dynamic dimension, like when cinema has been discovered after the reign of photography. Animated molecules took the place of immobile structures. Their work over the past three decades is at the origin of an incredible variety of molecular machines with a few of them described in this highlight review.

Our strategy for designing new molecular machines uses both a biomimetic[2] and a technomimetic[3] approach. Biomimetic molecules are designed by taking inspiration from Nature, where a considerable number of biochemical machineries like rotative ATP synthase[4] are used in all the living systems, to imitate (mimic) natural functions or materials. Motors and gears have been designed by using simplified structures to give access to artificial molecular motors and gears. A technomimetic molecule is a compound designed to resemble macroscopic machinery at the molecular level, also transposing the motions that these objects are able to undergo. According to this definition, technomimetic molecules can be also biomimetic but in that case, we usually define the molecule as a biomimetic entity. For instance, in the last decade, we synthesized rolling prototypes like nanowheels,[5] wheelbarrows[6] and nanocars.[7]

Operating on a single molecule in charge of the machinery is the physical limit of miniaturization. On a surface, the mechanical properties of a single molecule are essentially classical so its manipulation with a scanning tunneling microscope (STM) tip is a convenient way adapted to the classical motions we are willing to control. When a statistical amount of molecular machines is studied in solution or in a crystal, it is possible to obtain a lot of information through spectroscopic or crystallographic techniques but these are the result of the average behavior of a very large assembly of molecules. To reach the reality of only one molecule, we need to address and measure the mechanical properties on a single molecule.[8] Also, the ultimate miniaturization of mechanical machines is reached when the targeted function is realized with the minimum amount of matter, i.e. a single molecule. This is what we achieved by working with a STM. The molecules described here have been designed to be adsorbed on a surface and then studied individually.

In this highlight review, we will present our contribution to the field of biomimetic and technomimetic molecular machines with prototypes of gears, motors, wheels, wheelbarrow and nanocars.

1. Biomimetic Machines: Molecular Motors and Gears

1.1 Synthetic molecular motors

Among the world of machines, a motor is a machine which consumes energy to produce work repetitively and progressively in a system via a unidirectional and controlled movement of one of its parts.[9] The inspiration of such motors comes both from the macroscopic world where motors are very common and from Nature with the fascinating machinery of muscles[10] for translational motors or ATP synthase[4] for rotating motors. Some very elegant examples of molecular rotary motors have already been described but they have been studied collectively and have in general many degrees of freedom.[11] There are basically three families of motors depending what kind of energy is provided to the system. As energy source, most of the motors are using a chemical energy i.e. energy coming from chemical's transformations or light and only a few are using electrons. Biomimetic or technomimetic strategies are not linked to a specific source of energy. In our research, we use the tip of the Scanning Tunneling Microscope (STM) to very locally provide electrons to the molecule we want to rotate. The molecules developed in our group have been designed with the intention to be studied individually with a STM to avoid to have only access to the average behaviour of an assembly of molecules. This implies our target molecules to be as rigid as possible in the chemical world and have minimal degrees of freedom in order to be manipulated on a surface with a maximum control on their motion.

1.1.1 Inspiration from Nature: ATP Synthase

Each human being consumes an average of 40 kg of adenosine triphosphate (ATP) per day, as a source of energy released by the exergonic hydrolysis of ATP mediated by various ATPase enzymes to give adenosine diphosphate (ADP) and phosphate (Pi). Synthesis of ATP and thus storage of energy takes place according to the reverse reaction, i.e. phosphorylation of ADP. The biological machinery where this process occurs is ATP synthase,[4] an enzyme present in the cell membrane (Figure 1). The source of energy is the trans-membrane proton concentration gradient, that is transformed into chemical energy in the additional phosphate bond.

As shown on Figure 1, ATP synthase is constituted of two parts: the first one, called F_1, is in the extracellular medium whereas the second, called F_0, is incorporated in the membrane. F_0 is composed of a stator (*a* and *b* units) and of a mobile part, the rotor, constituted of 10 to 12 proteic subunits (*c*) depending on the cells. In the presence of a trans-membrane proton concentration gradient, a flow of protons occurs at the interface between *a* and *c* domains through the successive protonation - rotation - deprotonation of *c* subunits. Indeed, when a proton is fixed on a negatively charged amino acid of subunit *c*, this subunit is neutralized and moves away from the positively charged subunit *a* towards the membrane due to its less polar environment. Repetition of this process with all the *c* subunits leads away the whole rotor, and deprotonation of *c* subunits occurs after a complete turn, with the liberation of protons in the other compartment. The rotor which is a proton-fueled turbine, extends into an axle (γ) in the F_1 part, and the movement of this axle induces a conformational change of the three $\alpha\beta$ subunits, thereby triggering the synthesis of ATP.

It is important to note that the structure of ATP synthase, and in particular of the *a* and *c* units, imposes a unidirectional motion of the rotor. Interestingly, the reverse reaction, i.e. the hydrolysis of ATP to ADP, can also be mediated by the same enzyme with a rotation in the opposite direction, leading to pumping of protons against the electrochemical gradient.

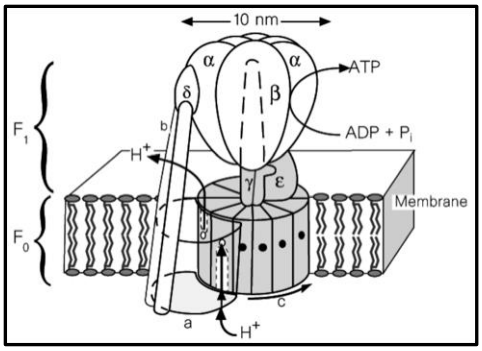

Figure 1. *ATP synthase incorporated in a membrane, with a trans-membrane proton concentration gradient leading to the synthesis of ATP.*

Inspired by this high-performance natural device, chemists challenged themselves to reach the same result on a smaller scale. Indeed, this biomachine is constituted of different biological macromolecules with a total size of 10 nm in diameter and about 25 nm in length (> 500 000 Daltons) which is much larger than the usual molecular size. In our group, we designed[12] a molecular motor about one order of magnitude smaller in each dimension and 300 times lighter with a molar mass of 1882 g.mol^{-1}.

As exemplified by ATP synthase, a key parameter for the possible recovery of useful work is the organization of the assembly of motors. The efficiency of this enzyme is for instance directly related to its trans-membrane location, since compartmentalization is a prerequisite for the creation of an electrochemical gradient. In this context, our goal was to study surface-mounted artificial motors, so as to obtain an identical orientation within the assembly of motors as opposed to machines studied in solution. All the artificial rotary molecular motors designed and synthesized in our group are thus composed of an azimuthal rotor, parallel to the surface, and of a stator specifically functionalized to provide tight anchoring on surface. Both rotor and stator, featuring rigid scaffolds, are coordinated to a central metal atom which acts as a rotation axle. After synthesis and deposition on surface, such ruthenium- and europium-based motors were submitted to a suitably oriented electrical field with the STM to induce rotary motion.

1.1.2 An organometallic piano-stool molecular motor

The first family of motors reported by our group was directly inspired by the motion of the rotor subunit in ATP synthase, triggered by coulombic interactions with its environment. Indeed, the motor was designed to be tightly anchored on a surface via its stator subunit, and to be located between two nanoelectrodes (i.e. in a nanojunction).[13] The top C_5-symmetrical rotating subunit comprised a central core surrounded by five rigid arms, each terminated by an electroactive ferrocene group (Fc) selected for its stability at the +II and +III oxidation states and the full reversibility of the related redox processes. As depicted in Figure 2, oxidation of the ferrocene unit located near the anode would release a positively charged ferrocenium, which would subsequently be repelled by coulombic interaction and driven away towards the cathode. This motion would bring the next ferrocene group close to the anode for an oxidative process, while the ferrocenium group would approach the cathode and be reduced to regenerate a neutral ferrocene. As a result, the successive oxidation-reduction cycles would drive the rotation, and electrical energy would be converted into a rotary motion. However, it is important to note that unidirectional motion can only be achieved in this system provided the two possible paths from

anode to cathode are different, i.e. if this horizontal setup is dissymmetric. This condition would for instance be reached by placing the motor dissymmetrically between the two electrodes.

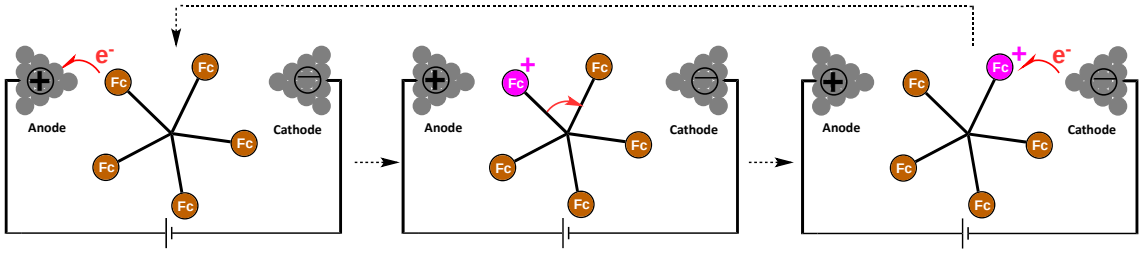

Figure 2. *Electrochemical actuation of the motor between two electrodes.*

From a structural point of view, motors belonging to this family are all based on organometallic piano-stool ruthenium(II) complexes.[13] The C_5-symmetrical rotor subunit is a penta(aryl)cyclopentadienyl ligand, carrying rigid arms terminated by ferrocene groups. As stator, a rigid hydrotris(indazolyl)borate ligand was selected for its ability to lift up the ruthenium center (and thus the rotor) from the surface via the location of nitrogen coordinating sites.[14] On the opposite side, this tripodal ligand was equipped with three functional groups allowing strong adsorption on surface, thereby preventing translation, rotation and rocking motions of the stator during scanning probe microscopy studies.

A family of molecular motors was synthesized according to this design, with esters as anchoring groups[15] compatible with the insulating oxide surfaces used as a support for nanoelectrodes (Figure 3).[16] Keeping the ferrocene terminal groups, the internal structure of the arms was in particular varied, with the introduction of organic[16b] and organometallic[16a] insulating spacers to prevent undesired intramolecular electron transfers. Unfortunately, in spite of the impressive technological advances in the field of surface physics, addressing such a single-molecule motor within a nanojunction composed of nanoelectrodes is still impossible nowadays, due to the size difference between the smallest nanoelectrodes and the molecular motor. The distance between the two electrodes could be as small as 45 nm, but the height of such nanojunction would be one order of magnitude higher than the molecule possibly leading to direct electron transfers between electrodes without crossing the molecular motor.

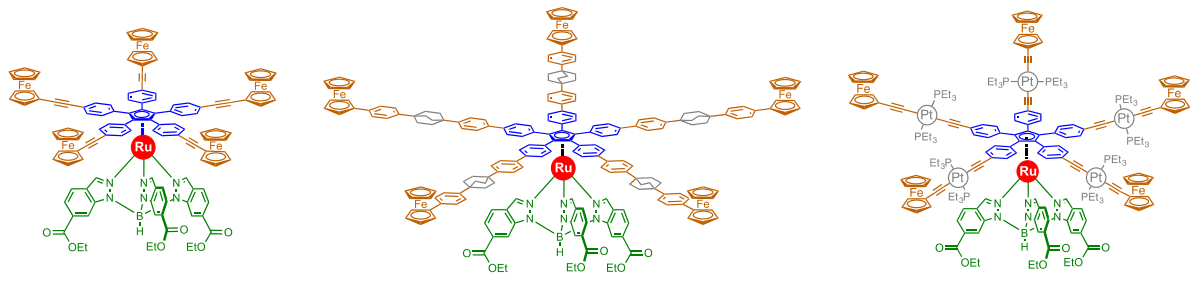

Figure 3. *Molecular motors bearing five ferrocene terminal groups. Molecules in the center and in the right include bicyclooctane and platinum spacers (in grey) to insulate the extremity of the arms to minimize intramolecular electron transfers.*

In the meantime, it was envisioned as an alternative strategy to place the molecular motor in a vertical setup, with the tip of the STM acting as a localized atomic-scale electrode and the metallic conductive surface being considered as an infinite electrode. In such setup, the STM tip is used as a source of electrical energy but also to monitor the rotary motion of the motor. Since the scanning tunneling microscopy is not a time-resolved technique, a possible movement can only be evidenced by comparison of the images obtained before and after triggering the rotation. It thus appeared necessary to lower the symmetry of the upper rotating part, not only as a probe for rotation on STM images but also to achieve unidirectional rotation.[17] Theoretical studies were undertaken to compare the ground-state potential energy profile of similar ruthenium-based motors carrying symmetric and dissymmetric rotors and assess their ability to undergo unidirectional rotation.[18] As depicted on Figure 4, in the dissymmetric structure, one ferrocene group was substituted with a methyl group, to afford one sterically and electronically different arm. Since a conductive surface is necessary for STM studies, the ester anchoring groups located on the stator were replaced with thioether groups, particularly suitable for coinage metals. The ground-state potential energy profile of each prototype adsorbed on Au(111) was calculated (semi-empirical ASED+ and DFT) methods as a function of the rotation angle of the rotor subunit.

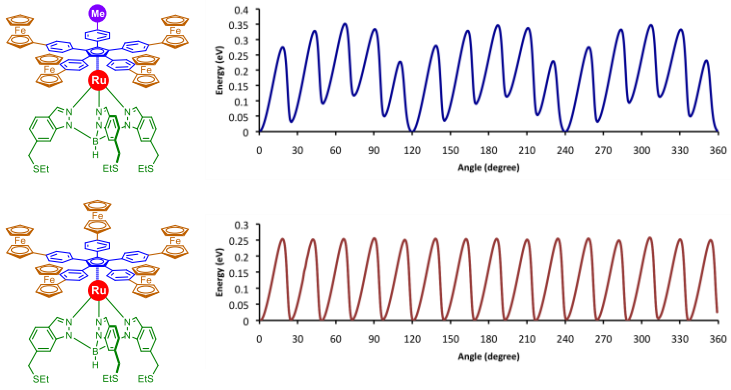

Figure 4. *Effect of desymmetrization on the shape of the ground state potential energy curve during the rotation along the Ru-Cp axle.*

For the symmetric motor (Figure 4, bottom), the potential energy profile features 15 wells, in good agreement with the combined C_5 and C_3 respective symmetries of the rotor and stator. The saw-tooth shape of the curve is related to interactions between the phenylene groups in the rotor's arms and the indazole rings of the stator. However, this feature is not sufficient to achieve unidirectional motion as the height of the activation barrier remains constant (0.25 eV). In the case of the dissymmetric motor (Figure 4, top), 15 local minima are present and an additional periodicity of 120° is now observed as a result of the introduction of one truncated arm. The saw-tooth profile is in this case characterized by variable rotation barriers in the 0.22-0.35 eV range, implying that one direction of rotation is favored at each local minimum. According to these theoretical studies in the ground state, dissymmetrization of the structure of the rotor may lead to unidirectional rotation and this interesting candidate was thus synthesized[12,19] and deposited on a Au(111) surface. STM imaging of single molecules at 77 K indicated that this motor (Figure 4, top) exhibit non-directional free rotation at that temperature due to Brownian motion. When the temperature is lowered to 5 K, rotation stops as can be seen by the dissymmetric shape of the rotor on the STM image.[18] At that temperature, it was shown that a voltage pulse applied with the STM tip on one of the arms of the motionless rotor triggers its rotation, and successive excitations on the same arm lead to stepwise unidirectional rotary motion. More interestingly, we demonstrated that

the clockwise or counter-clockwise direction of rotation is directly controlled by the nature of the arm excited by the STM tip and can be inverted at will (Figure 5).

We thus developed the first reversible electron-fueled molecular motor, based on an organometallic piano-stool ruthenium complex. It is important to mention here that, contrary to the initial concept, electron transfers in this vertical setup are too fast for any redox process to occur in the electroactive groups. Rotation of the molecular motor is triggered by inelastic electron energy transfer through low-lying excited states, with a directionality imposed by the shape of the potential energy profile in these excited states. Studies are currently underway to estimate the motive power of this molecular motor.

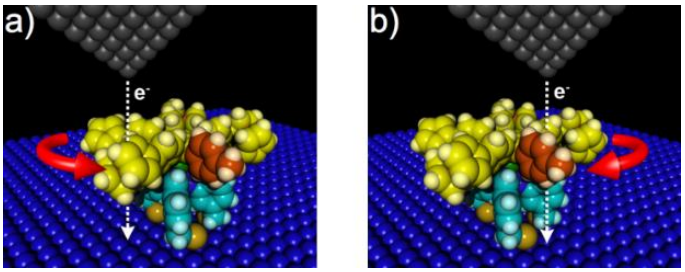

Figure 5. *CPK representation of the motor undergoing unidirectional rotation, depending on the position of the STM tip. a) tip above a ferrocene group inducing a counterclockwise rotation. b) tip above the tolyl group inducing a clockwise rotation.*

1.1.3 A double-decker europium molecular motor

Another type of azimuthal molecular motor was next targeted, with the aim of obtaining a controllable self-assembled monolayer to be studied as a collective assembly on surface.

An heteroleptic europium(III) double-decker complex was designed, incorporating a naphthalocyanine stator and a porphyrin rotor (Figure 6, left). The naphthalocyanine stator was functionalized with eight thioether anchoring groups, bearing long alkyl chains to tune the distance between motors within the self-assembly. The porphyrin stator was functionalized on opposite meso positions with donor butoxyphenyl and acceptor cyanophenyl groups, respectively. The upper rotating subunit was thus dissymmetric, with a donor-acceptor character highlighted by a permanent electric dipole moment of 8 D.

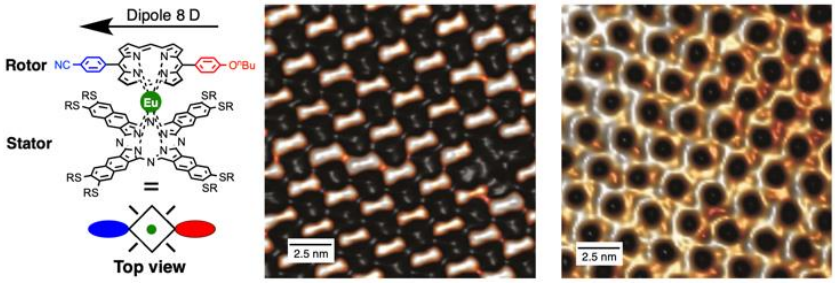

Figure 6. *Double-decker molecular motor based on a europium(III) complex with its schematic representation used in Fig. 7 (left) and STM images at low voltage (center, - 0.55 V, 0.2 nA, the molecules are not rotating and appear as rod) and high voltage (right, 1.6 V, 0.2 nA, the molecule are all rotating).*

The target compound was synthesized[20] and deposited by sublimation on Au(111). At 5 K, it was observed by STM that the individual rotors undergo free random rotation, which can be accounted for by very low rotation barriers in such double-decker complexes. Alternatively, deposition on Cu(111) afforded highly ordered self-assembled two-dimensional domains exhibiting hexagonal symmetry (Figure 7).[21] Strikingly, at 80 K, the motors within this network are motionless at low bias voltage, also revealing a parallel alignment of the electric dipoles thereby suggesting the existence of intermolecular interactions (Figure 6, center). At higher voltage, all the motors are rotating (Figure 6, right) and a deeper analysis revealed that there exists a voltage for which a synchronized switch of a large domain of rotors can occurs around a bias voltage of 1.2 V. This simultaneous collective switching when applying an electric field from the tip of a STM is triggered by dipolar interactions within the hexagonal ferroelectric network of molecular rotors, thereby highlighting intermolecular communication between single molecules of the network.

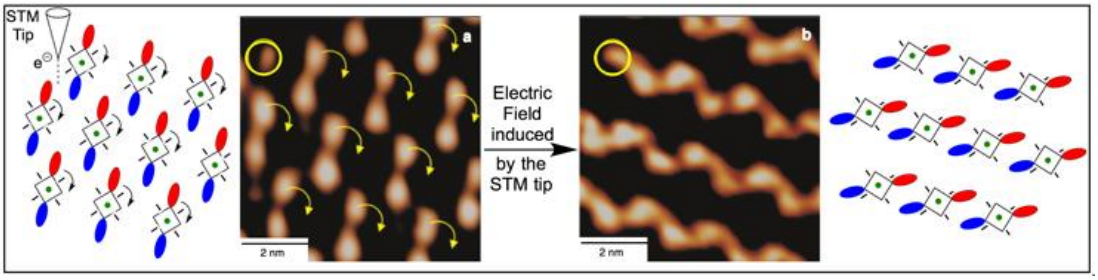

Figure 7. *Synchronized switch at a bias voltage of 1.2 V. Images and respective schematic representations before (a) and after (b) the application of an electric field induced by the STM tip (position of the tip shown by a yellow circle).*

We thus achieved the controlled and synchronized rotation of single dipolar molecular motors within a self-assembled monolayer, which opens the ways to the operation of assemblies of molecular machines packed on surface using an electrical stimulus.

Following our work in the field of molecular motors, for which an electrical stimulus induced the controlled rotation of single molecules, we next aimed at exploiting the work provided by such motors, in particular via a transfer of the rotary motion to neighbouring molecules. This implies first to get a deeper understanding of the mechanical transmission of motion at the molecular scale which we envisioned to study on surface trains of molecular gears mechanically actuated by the tip of a STM.

1.2 Synthetic molecular gears

Gears have long been considered as a human invention, with the oldest known machine involving gearing mechanisms being the Antikythera machine which dates back to the Hellenistic period. However, gearing patterns are found in the animal kingdom and functional micrometric gears were unexpectedly discovered recently in the insect's world.[22]

1.2.1 Natural micrometric gears in the insect's world

Burrows and Sutton studied the nymphs of the planthopper *Issus coleoptratus*, belonging to a class of insects known for their impressive jumps induced by fast and powerful movements of their hind legs. These authors disclosed in 2013 that a curved strip of 10-12 gear teeth is incorporated in the exoskeleton of these insects' legs, each tooth being 9 µm thick and 15-30 µm wide as observed by Scanning Electron Microscopy (Figure 8).[22] By means of high-speed video, the study revealed that both cogwheels are engaged to each other during the preparation of the jump and the propulsion, which allows a synchronous movement of the legs on a µs scale. Indeed, both legs are mechanically coupled via this gearing mechanism, which leads to higher synchronization of their movement as compared to simple neural excitation. Interestingly, the teeth are dissymmetric, thereby having only one direction of powered rotation.

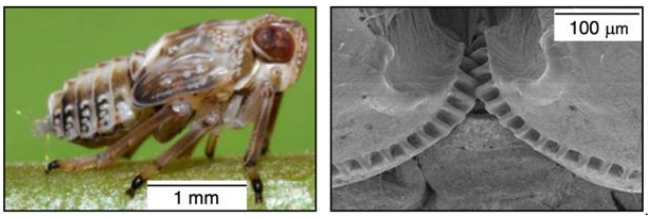

Figure 8. *The nymph of the planthopper Issus coleoptratus (left) and a Scanning Electron Microscopy image of the intricated micrometric gears located on the hind legs (right). From Ref 22. Adapted with permission from AAAS.*

1.2.2 Design of nanometric gears to be studied on-surface as single molecules

As early as in 1980, Mislow[23] and Iwamura[24] independently reported the first examples of molecular bevel gears studied in solution and featuring intricated triptycene moieties. In 2012 Siegel *et al.* synthesized the first molecular spur gears after careful molecular design and DFT studies to optimize the inter-axle distance, highlighting the importance of this parameter in molecular gearing mechanisms.[25] Very recently, Shionoya *et al.* reported a Pt(II)-centered molecular gear, wherein the two azaphosphatriptycene cogwheels are very elegantly disengaged or engaged via photo- or thermally-induced *cis-trans* isomerization, respectively.[26]

In contrast with molecular gears studied in solution, solely allowing intramolecular processes, intermolecular gearing becomes possible on a supporting surface, used to maintain the relative orientation of rotation axles and the distance between the cogwheels. To the best of our knowledge, intermolecular gearing on surface was demonstrated for the first time in 2007 by Moresco et al. in a rack and pinion device.[27] Indeed, when a single star-shaped molecule of penta(*p-tert*-butylphenyl)-(*p-tert*-butylpyrimido)benzene was moved laterally via STM manipulation along the edge of an island of the

same molecules on Cu(111), rotation of the single molecule was evidenced on successive STM images by following the relative position of the *N*-tagged arm. Further studies at the single molecule scale on Au(111) revealed that it is possible to achieve a stepwise rotation of such star-shaped molecule when mounted on an atomic scale axis.[28] Unfortunately all attempts to transfer the rotary motion to a neighbouring molecule proved unsuccessful, since diffusion of the molecules precluded the desired motion. This seminal work thus underlines the importance of identifying appropriate rotation axles for intermolecular gearing to take place on surface. In this context, one of the strategies relies on a metallo-organic rotation axle, in which the ligand provides tight anchoring on the surface through specific functional groups, and the metal ion acts as a ball bearing. It thus appeared that the architecture of the previously-reported ruthenium-based motor would be particularly suitable, especially as it was observed during STM experiments that lateral manipulation of such single ruthenium complexes is possible at 77 K when molecular diffusion is frozen at 5 K. This would thus allow the construction of trains of gears of various lengths at 77 K, with finely tuned inter-axle distances, and subsequent cooling to 5 K would maintain the spatial arrangement of molecules during gearing experiments.

In these experiments, the STM tip is used as a source of mechanical energy to induce the rotary motion of the first cogwheel by pushing on one of the teeth (Figure 9). If the gearing mechanism occurs, the propagation of the rotary motion through the alignment of molecules will then be evidenced by comparing the STM images of the initial and final states, meaning that in our initial design one of the teeth has to be chemically or sterically tagged.

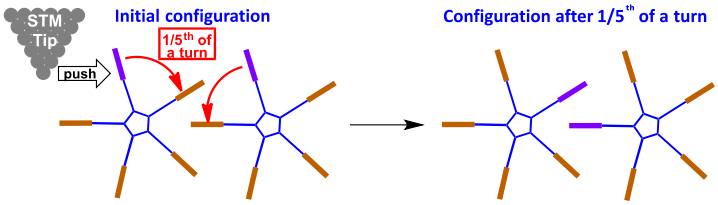

Figure 9. *Principle of the motion transmission through a molecular gear train actuated by a STM tip.*

1.2.3 Molecular gears with 1D and 2D paddles

Some of the specifications for an intermolecular transfer of rotary motion at the molecular scale are still open questions. Indeed, it is obvious that the presence of a rotation axle, the inter-axle distance and the teeth interlocking are major parameters, but the influence of the nature and structure of the teeth is still difficult to anticipate.

A first star-shaped ruthenium complex involving four biphenyl teeth and one chemically-tagged phenylpyridine tooth was thus designed (Figure 10, left). Unfortunately, theoretical studies carried out on two such interacting molecular gears showed that a vertical deformation of the teeth due to their relative flexibility can lead to gear slippage, thus preventing any gearing mechanism.

In order to disfavor gear slippage, it is now envisioned to increase the size of the teeth, moving from 1D-biphenyl teeth to larger 2D teeth, such as pyrene-derived units. Due to steric hindrance, these flat paddles would lie perpendicular to the central cyclopentadienyl ring and even if vertical deformation occurs, the contact surface between two contiguous paddles should be sufficient to propagate the rotary motion. The synthesis of this new generation of molecular gears carrying 2D-paddles is currently underway.

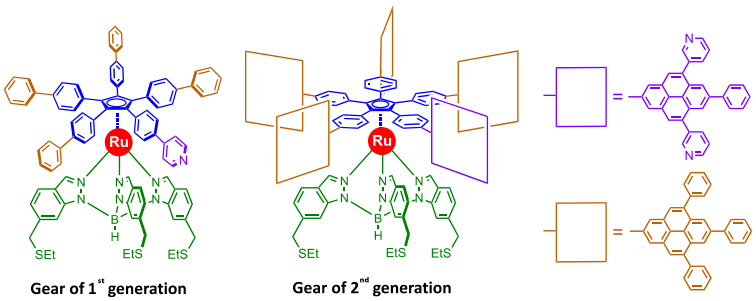

Figure 10. *Evolution of ruthenium-based molecular gears: from 1D arms (1st generation) to 2D paddles (2nd generation).*

2. Technomimetic Machines: Wheels, Wheelbarrows and Nanocars

Controlled rotational motions are very important not only for molecular motors but also more generally for technomimetic-like molecule such as weels or more complex nanovehicles like a two-wheels nanowheelbarrow or four-wheels nanocars. Nanovehicles are molecular machines basically composed of a chassis and wheels,[29] typically one or two for a barrow,[30] four for a nanocar[31] or more for nanotrucks and nanotrains.[32] In order to build such nanovehicles, the choice of the wheel is a very important parameter. It must allow the entire functionalized molecule to move easily on the surface by its rolling motion. As pioneers in the field, we proposed triptycenes[33] to act as rolling elements and synthesized the first nanovehicle[30] while two years later Tour's group reported a family of nanovehicles[34] using [60]-fullerenes wheels. Let us start with an axle terminated with two wheels.

2.1 A dimer of triptycenyl wheel

Triptycene[35] is a very attractive building block since its symmetry and rigidity allow it to be exploited on surfaces. Several examples of molecular devices have been reported where the key fragment is based on triptycene, such as molecular gears,[36,25] motors,[11a] gyroscopes[37] and brakes.[38]

Our prototype of a wheel dimer is the bisethynyltriptycene presented Figure 11. Its deposition on a Cu(110) surface has been achieved very cleanly by sublimation under high vacuum. On the image obtained, each bright lobe corresponds to one triptycene and therefore, a pair of lobes constitutes the image of a dimer as confirmed by calculations.[39] No fragmentation or decomposition has been observed confirming their interest as STM-compatible fragments. Molecules were deposited and studied at 5K under ultra-high vacuum. Unidirectional rotation of the wheel by inducing the translation of the molecule with a step-by-step rotation of the wheels upon pushing with the STM tip was demonstrated for the first time.[39]

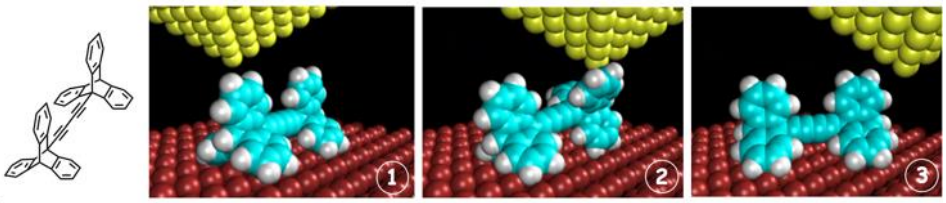

Figure 11. *Chemical structure of a dimer of wheels and its motion under the pushing of a STM tip. (1) the tip approaches the molecule, (2) the tip induces the 120° rotation of one triptycene wheel and (3) the tip continues its motion.*

The tip was moved across the molecular axle at constant height, while the tunneling current was recorded at the same time. The motion has been understood thanks to the study of the tunneling current recorded at constant tip height during the motion. In the case of rolling motion, a "hat-shaped" signal appears while sliding of the molecule on the surface induced a periodic electric current directly linked with the periodicity of the surface. Typically, one wheel is left in its initial position while the other one rotates and in a few cases the rolling of both wheels has been observed. This behavior seems to very be highly dependent of the precise shape of the tip.

Even though rotation is the preferential motion in the macroscopic world, rolling of a wheel at the nanoscale has been more difficult to obtain. Behind the molecule selected to act as a wheel, the choice of the surface is very important. For instance Cu(100) is too flat. A more corrugated surface such as Cu(110) is essential to allow the rolling of a wheel because according to DFT calculations, the angle of two phenyl rings of the triptycene is not 120° anymore like calculated for the molecule without Cu surface, but 140° to maximize their interactions with the metallic surface. The characteristic mechanisms of hopping and rolling motions are reflected in different molecular displacements.

This was the first direct proof of the rolling motion of a wheel which encouraged us to develop more complex nanovehicles with two or four wheels. Extension of this work on silicon-based surfaces has also shown some very interesting motions with a good mobility and the control of the directionality[40] at the nanoscale at room temperature which is very important for practical applications of molecular machines.[41]

2.2 A molecular wheelbarrow

When we started in the field, recent advances in the imaging and manipulation of single molecules with LT-STM stimulated us to synthesize technomimetic nanoscale molecular objects exhibiting unique mechanical properties like this molecular wheelbarrow.[6] In the case of a macroscopic wheelbarrow, pushing the wheelbarrow results in the translation of the molecule with simultaneous rotation of the wheel. Our molecular analog has been design to achieve such motion at the molecular scale. Its skeleton is made of a Polycyclic Aromatic Hydrocarbons (PAHs) which, due to its rigidity, can be easily manipulated by the STM tip. In addition they can provide us with a potential cargo zone able to transport atoms or small molecules on surfaces. They are also relatively resistant to the deposition techniques which are basically based on sublimation of the molecule upon heating.

The wheelbarrow is constituted of two legs and two wheels connected to a polycyclic aromatic hydrocarbon platform (Figure 12). The two legs (in green) are 3,5-di-*tert*-butylphenyl groups which have been been shown to have the phenyl groups nearly perpendicular to the main aromatic board.

Moreover, the *tert*-butyl groups connected to the PAHs are used to increase organic solubility and are easily observed by STM techniques, inducing a good contrast in the image. The two 4-*tert*-butylphenyl groups were selected to play the role of handles (in blue) for subsequent manipulation with the tip of the microscope. The second axle is equipped with two 9-triptycenyl groups acting as wheels (in red). Figure 12 shows one of the possible conformations of the molecule obtained by semi-empirical calculation and the two three-cogged wheels which can freely rotate along the axle due to the acetylenic spacers.[42]

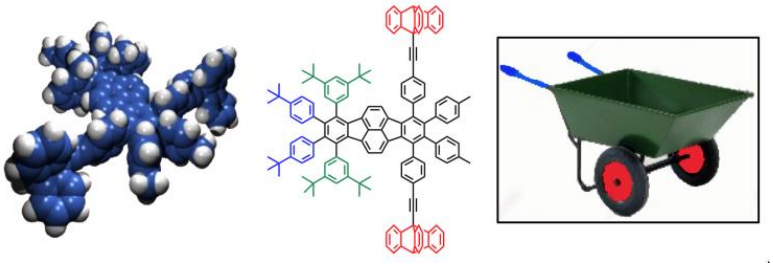

Figure 12. *CPK model showing the minimum energy conformation of the molecular wheelbarrow (left), chemical structure (center) and its macroscopic analog (right).*

Standard sublimation techniques usually used to depose molecules in the STM did not give any positive results due to the large weight of the molecule (1802 $g.mol^{-1}$). In particular, the presence of the triple bonds tends to induce decomposition at the required high temperature, yielding some rearrangement reactions on the surface.[43] Using some fast heating techniques, we successfully imaged a few intact molecular wheelbarrows on a Cu(100) surface as shown in Figure 13 and identified by comparison with calculated images.[44]

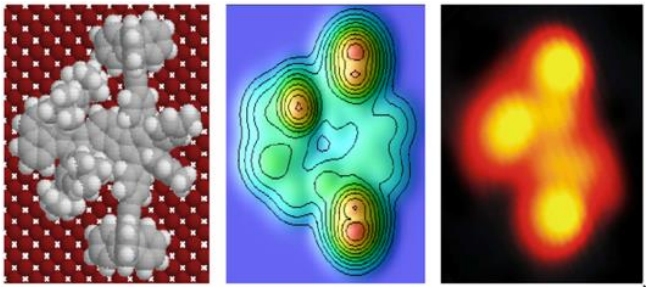

Figure 13. *The molecular conformation obtained by interacting the molecule on the surface (left), the corresponding calculated image using ESQC (center) and the experimental STM image of the molecular wheelbarrow on Cu(100) (right) at 5K under UHV conditions.*

Manipulation at 5K resulted in a change of conformation of the molecule which confirmed the molecularity of the observed object but unfortunately, lateral motion of the wheelbarrow was not achieved. This was explained by a very strong interaction between the molecule and the metallic surface of copper mainly due to the large aromatic planar structure which can interact with the surface.

To obtain more mobile molecules, we decided to extend our studies to four-wheel molecules, which we named nanocars.

2.3 A planar four-wheel nanovehicle

The polyaromatic fragment used as chassis in the molecular wheelbarrow was too short to sterically accommodate four wheels. Therefore, we have developed the synthesis of a larger chassis based on a perylene unit (in blue).[7]

As shown on Figure 14, the extended perylene polyaromatic contain eight *tert*-butyl groups to enhance the solubility of this system and again the four triptycenyl wheels (in red) were connected along the two axles thanks to the ethynyl spacers which ensure a very low rotation barrier.[42]

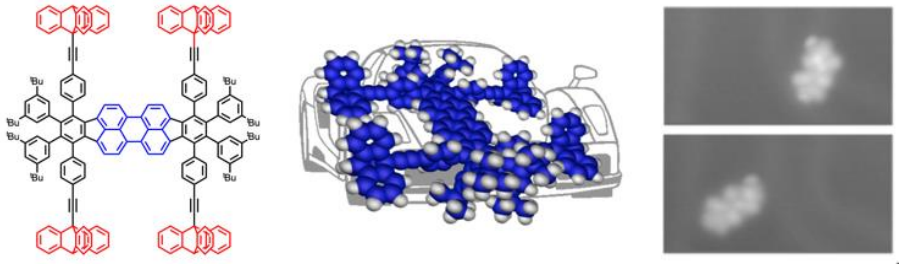

Figure 14. *Chemical structure of the nanocar (left), its CPK model showing its planar conformation (center) and two STM image showing the pushing of the molecule on a Au(111) surface.*

This nanovehicle has been deposited on Au(111), however, due to its planarity and the resulting high interaction of the polyaromatic chassis with the surface, it has been very difficult to move it.[45] Only a few non-reproducible movements have been obtained by pushing with the tip of the STM (5K, under UHV conditions).

To increase the mobility of such large molecule, we designed a similar nanocar build around a curved chassis which would have a lower interaction with the surface.

2.4 A curved four-wheel nanovehicle

To decrease the interaction of the molecule with the surface, our strategy has been to use a highly curved polyaromatic chassis. During the synthesis of the planar nanocar, it appeared that if we decreased the number of *tert*-butyl groups on the precursor from two at the meta positions to one at the para position, dimerization of the half-chassis following the Scholl-type oxidative coupling gave an overcyclized perylene platform bearing a fragment of hexa-peri-hexabenzocoronene (in blue) on each extremity of the molecule. This was due to a smaller steric allowing different phenyl rings to be co-planar during the reaction, which was not the case with the former precursor having eight *tert*-butyl groups.[7]

As shown on Figure 15 (center), the overcyclized chassis has a curved shape according to a geometric optimization of this second generation nanocar. Like in fullerene derivatives, this geometry can be explained by the presence of alternating five and six-membered rings in the polycyclic aromatic hydrocarbon platform.

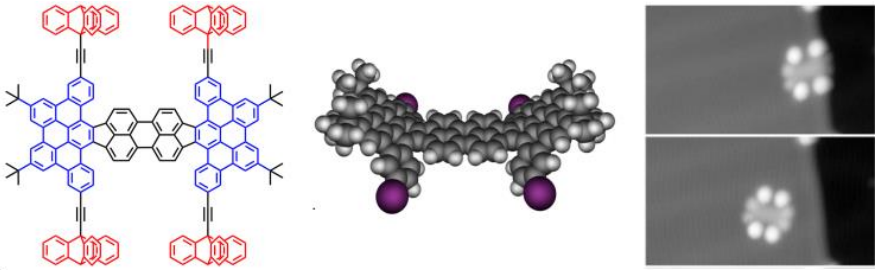

Figure 15. *Chemical structure of the nanocar (left), CPK model of the chassis before the connection of the four wheels showing its highly curved conformation (center) and two STM image showing the pushing of the molecule on a Au(111) surface.*

As expected, the curved nanocar bearing only four *tert*-butyl groups is much less soluble than the planar one which explains the lower yield and difficulties to achieve the two last steps with satisfying yields. Also, the spectroscopic properties are very different, the planar nanocar is pink while the curved one is dark green.

STM study of this molecule gave a very clear image compared to the planar one with a very high contrast for the four triptycene wheels.[46] This is due to a smaller interaction of the curved polyaromatic chassis and this molecule has indeed shown a much higher mobility on the Au(111) surface under the pushing or pulling, leading to its selection for the first nanocar race.[47]

2.5 Participation to the first nanocar race

Due to its green colour, we named our curved nanocar "the green buggy". The last week-end of April 2017, six teams from three continents competed in Toulouse with their racers. Three nanocars from Austria, France and the USA were technomimetic, incorporating wheels, and the three other models from Germany, Japan and Switzerland were not, since they did not use wheels.[48] It must be noted that there is no need at the nanoscale to have technomimetic-based nanocars with wheels as a prerequisite for mobility. For instance, the very elegant japanese nanocar similar to a butterfly[49] or the winner of the race, the swiss dragster,[50] both lacked wheels fragments. According to the published rules, the common surface used was Au(111) with a track of 100 nm long including two turns.

The french nanocar has the advantage of being very robust. After deposition by sublimation, it has been identified on the surface. As shown in Figure 16, the triptycene wheels appear as very bright spots compared to the central polyaromatic core.

To move it directionally we explored two strategies. First, we tried to find a way for an electronic excitation to induce the movement but we failed. Since direct pushing with the STM tip was forbidden by rule, an alternative strategy has been to pull the molecule which allowed us to cover an impressive distance of 25 nm in a few seconds. Unfortunately, the jury refused to homologate our pulling strategy and we were disqualified from the race, remembering the moto from Pierre de Coubertin, the creator of the modern Olympic games, which emphasizes that "the importance is to participate". Anyway, we have been very satisfied to receive the "prize of elegance" thanks to the very smart STM images obtained for our nanocar.

Figure 16. *The french team (G. Rapenne, C. Kammerer and C. Durand) with their official dark green t-shirt received the "prize of elegance" from the jury. In the flask the powder of the '"green buggy" and its STM image superimposed with the chemical structure. The four luminous spots fit perfectly with the position of the four wheels.*

In Spring 2021, a second Nanocar race will take place with thirteen competitors already registered beyond them a franco-japanese team composed of the authors of this highlight review. We designed a new dipolar nanocar and its synthesis is underway in NAIST (Japan) before to have its mobility and driving ability tested on a Au(111) surface in CEMES (France).

Conclusion and perspectives

Biomimetic and technomimetic strategies are complementary and they both gave rise to various nanomachines with controlled molecular motions. Unfortunately the extremely low operating temperature, typically 5 K, prevents any kind of practical applications and our strategy is now to operate at higher temperature. In the case of molecular motors, from our ruthenium complex to the europium double decker we already moved from 5 to 80 K with some interesting synchronized and collective motions.

Although some progress has been made, it is still a long way to practical applications but there is already a lot to learn from the behaviour of single molecules. For instance, transporting in a controlled way atoms or molecules on a surface is a challenging topic for matter transport at the nanoscale. For that last purpose our nanovehicles are of great interest since they provide an appropriate shape to act as an efficient cargo zone.

Acknowledgements

This work was supported by the University Paul Sabatier (Toulouse, France) and the Centre National de la Recherche Scientifique (CNRS). It has received funding from the Agence Nationale de la Recherche (ANR) (ACTION project ANR-15-CE29-0005) and from the European Union's Horizon 2020 research and innovation programme under the project MEMO, grant agreement No 766864. This research was also partly supported by the JSPS KAKENHI Grant in aid for Scientific Research on Innovative Areas "Molecular Engine (No.8006)" 18H05419. We are also grateful to the researchers who participated in all the work discussed here and whose names appear in the references, and in particular

the talented PhD and Post-doctoral students who achieved the synthesis of these systems: Alexandre Carella, Guillaume Vives, Henri-Pierre Jacquot de Rouville, Roman Stefak, Romain Garbage, Agnès Sirven and Dr. Gorka Jimenez-Bueno, as well as Dr. Francesca Moresco, Dr. Leonhard Grill, Dr Sébastien Gauthier, Dr Corentin Durand and Prof. Saw-Waï Hla for STM studies, and Dr. Christian Joachim, Jorge Echeveria-Lopez and Dr. Xavier Bouju for theoretical calculations. Dr Colin Martin is also warmly acknowledged for his careful reading and improving of our manuscript.

References and Notes

1 a) J.-P. Sauvage, *Angew. Chem., Int. Ed.* **2017**, *56*, 11080. b) J. F. Stoddart, *Angew. Chem., Int. Ed.* **2017**, *56*, 11094. c) B. L. Feringa, *Angew. Chem., Int. Ed.* **2017**, *56*, 11060.
2 R. Breslow, *J. Biol. Chem.* **2008**, *284*, 1337.
3 G. Rapenne, *Org. Biomol. Chem.* **2005**, *3*, 1165.
4 J. E. Walker, *Angew. Chem. Int. Ed.* **1998**, *37*, 2308.
5 H.-P. Jacquot de Rouville, R. Garbage, F. Ample, A. Nickel, J. Meyer, F. Moresco, C. Joachim, G. Rapenne, *Chem. Eur. J.* **2012**, *18*, 8925.
6 G. Rapenne, G. Jimenez-Bueno, *Tetrahedron* **2007**, *63*, 7018.
7 H.-P. Jacquot de Rouville, R. Garbage, R. E. Cook, A. R. Pujol, A. M. Sirven, G. Rapenne, *Chem. Eur. J.* **2012**, *18*, 3023.
8 C. Joachim, G. Rapenne, *Top. Curr. Chem.* **2014**, *128*, 510.
9 C. Pezzato, C. Cheng, J. F. Stoddart, R. D. Astumian, *Chem. Soc. Rev.* **2017**, *46*, 5491.
10 a) I. Rayment, H. M. Holden, M. Whittaker, C. B. Yohn, M. Lorenz, K. C. Holmese, R. A. Milligan, *Science* **1993**, *261*, 58. b) For a review on artificial molecular muscles, see : F. Niess, V. Duplan, J.-P. Sauvage, *Chem. Lett.* **2014**, *43*, 964.
11 a) T. R. Kelly, H. D. Silva, R. A. Silva, *Nature* **1999**, *401*, 150. b) N. Koumura, R. W. J. Zijlstra, R. A. van Delden, N, Harada B. L. Feringa, *Nature* **1999**, *401*, 152. c) D. A. Leigh, J. K. Y. Wong, F. Dehez, F. Zerbetto, *Nature*, **2003**, *424*, 174. d) G. S. Kottas, L. I. Clarke, D. Horinek, J. Michl, *Chem Rev.* **2005**, *105*, 1281. e) S. Kassem, T. van Leeuwen, A. S. Lubbe, M. R. Wilson, B. L. Feringa, D. A Leigh, *Chem. Soc. Rev.* **2017**, *46*, 2592 and references therein.
12 G. Vives, G. Rapenne, *Tetrahedron* **2008**, *64*, 11462.
13 G. Vives, H.-P. Jacquot de Rouville, A. Carella, J.-P. Launay, G. Rapenne, *Chem. Soc. Rev.* **2009**, *38*, 1551.
14 C. Kammerer, G. Rapenne, *Eur. J. Inorg. Chem.* **2016**, 2214.
15 A. Carella, G. Vives, T. Cox, J. Jaud, G. Rapenne, J.-P. Launay, *Eur. J. Inorg. Chem.* **2006**, 980.
16 a) G. Vives, A. Carella, S. Sistach, J.-P. Launay, G. Rapenne, *New. J. Chem.* **2006**, *30*, 1429; b) G. Vives, A. Gonzalez, J. Jaud, J.-P. Launay, G. Rapenne, *Chem. Eur. J.* **2007**, *13*, 5622.
17 R. Stefak, A.M. Sirven, S. Fukumoto, H. Nakagawa, G. Rapenne, *Coord. Chem. Rev.* **2015**, *287*, 79.
18 U.G.E. Perera, F. Ample, J. Echeverria, H. Kersell, Y. Zhang, G. Vives, M. Grisolia, G., C. Joachim, S.-W. Hla, *Nature Nanotechnol.* **2013**, *8*, 46.
19 For an optimized synthesis of the tripodal ligand, see: G. Erbland, Y. Gisbert, G. Rapenne, C. Kammerer, *Eur. J. Org. Chem.* **2018**, 4731.
20 R. Stefak, N. Ratel-Ramond, G. Rapenne, *Inorg. Chim. Acta* **2012**, *380*, 181.
21 Y. Zhang, H. Kersell, R. Stefak, J. Echeverria, V. Iancu, U. G. E. Perera, Y. Li, A. Deshpande, K.-F. Braun, C. Joachim, G. Rapenne, S.-W. Hla, *Nature Nanotechnol.* **2016**, *11*, 706.
22 M. Burrows, G. Sutton, *Science* **2013**, *341*, 1254.
23 W. D. Hounshell, C. A. Johnson, A. Guenzi, F. Cozzi, K. Mislow, *Proc. Natl. Acad. Sci USA* **1980**, *77*, 6961.
24 Y. Kawada, H. Iwamura, *J. Org. Chem.* **1980**, *45*, 2547.
25 D. K. Frantz, A. Linden, K. K. Baldridge, J. S. Siegel, *J. Am. Chem. Soc.* **2012**, *134*, 1528.
26 H. Ube, Y. Yasuda, H. Sato, M. Shionoya, *Nature Commun.* **2017**, *8*, 14296.
27 F. Chiaravalloti, L. Gross, K.-H. Rieder, S. M. Stojkovic, A. Gourdon, C. Joachim, F. Moresco, *Nature Mater.* **2007**, *6*, 30.
28 C. Manzano, W.-H. Soe, H. S. Wong, F. Ample, A. Gourdon, N. Chandrasekhar, C. Joachim, *Nature Mater.* **2009**, *8*, 576.
29 C. Joachim, G. Rapenne, *ACS Nano* **2013**, *7*, 11.
30 G. Jimenez-Bueno, G. Rapenne, *Tetrahedron Lett.* **2003**, *44*, 6261.
31 T. Kudernac, N. Ruangsupapichat, M. Parschau, B. Macia, N. Katsonis, S. R. Harutyunyan, K.-H. Ernst, B. L. Feringa, *Nature* **2011**, *479*, 208.
32 G. Vives, J. M. Tour, *Acc. Chem. Res.* **2009,** *42*, 473.
33 C. Joachim, F. Moresco, G. Rapenne, G. Meyer, *Nanotechnol.* **2002**, *13*, 330.
34 Y. Shirai, A. J. Osgood, Y. Zhao, K. F. Kelly, J. M. Tour, *Nano Lett.* **2005**, *5*, 2330.
35 *Iptycenes chemistry from synthesis to applications*, ed. by C. F. Chen, Y. X. Ma, Springer-Verlag, Berlin, **2013**.
36 a) H. Iwamura, K. Mislow, *Acc. Chem. Res.* **1988**, *21*, 175.
37 C. Lemouchi, C. S. Vogelsberg, L. Zorina, S. Simonov, P. Batail, S. Brown, M. A. Garcia-Garibay, *J. Am. Chem. Soc.* **2011**, *133*, 6371.
38 a) T. R. Kelly, J. P. Sestelo, I. Tellitu, *J. Org. Chem.* **1998**, *63*, 3655. b) K. Nikitin, C. Bothe, H. Muller-Bunz, Y. Ortin, M. J. McGlinchey, *Organometallics* **2012**, *31*, 6183.
39 L. Grill, K. H. Rieder, F. Moresco, G. Rapenne, S. Stojkovic, X. Bouju, C. Joachim, *Nature Nanotechnol.* **2007**, *2*, 95.
40 X. Bouju, F. Chérioux,S. Coget, G. Rapenne, F. Palmino, *Nanoscale* **2013**, *5*, 7005.
41 F. Chérioux, F. Palmino, O. Galangau, G. Rapenne, G. *Chem. Phys. Chem.* **2016**, 1742.
42 S. Toyota, *Chem. Rev.* **2010**, *110*, 5398.
43 G. Rapenne, L. Grill, T. Zambelli, S. Stojkovic, F. Ample, F. Moresco, C. Joachim, *Chem. Phys. Lett*. **2006**, *431*, 219.
44 L. Grill, K.H. Rieder, F. Moresco, G. Jimenez-Bueno, C. Wang, G. Rapenne, C. Joachim, *Surf. Science* **2005**, *584*, 153.
45 Unpublished results
46 W.-H. Soe, C. Durand, S. Gauthier, H.-P. Jacquot de Rouville, C. Kammerer, G. Rapenne, C. Joachim, *Nanotechnology* **2018**, *29*, 495401.

47 H.-P. Jacquot de Rouville, C. Kammerer, G. Rapenne, *Molecules*, **2018**, *23*, 612.
48 G. Rapenne, C. Joachim, *Nature Rev. Mater.* **2017**, *2*, 17040.
49 W.H Soe, Y. Shirai, C. Durand, Y. Yonamine, K. Minami, X. Bouju, M. Kolmer, K. Ariga, C. Joachim, W. Nakanishi, *ACS Nano* **2017**, *11*, 10357.
50 R. Pawlak, T. Meier, *Nature Nanotechnol.* **2017**, *12*, 712.